ELSEVIER

International Journal of Mass Spectrometry 207 (2001) 41–55

International Journal of Mass Spectrometry

Production, dissociation, and gas phase stability of sodium fluoride cluster ions studied using electrospray ionization ion trap mass spectrometry

M.P. Ince, B.A. Perera, M.J. Van Stipdonk*

Department of Chemistry, Wichita State University, Wichita, KS 67260-0051, USA

Received 29 September 2000; accepted 8 December 2000

Abstract

A Finnigan LCQ-Deca™ was used to produce and characterize ions derived from solutions of sodium fluoride. As with sputtering experiments involving the same salt, electrospray produces an extensive series of positively charged cluster ions based on repeating units of NaF with a pendant Na cation. In addition, a series of doubly charged ions corresponding to multiple (NaF) units modified by the addition of two Na cations was observed. We found that the general peak intensity distribution in the mass spectrum of NaF was sensitive to the temperature of the heated capillary used in the LCQ to desolvate ions after formation by electrospray ionization. At temperatures greater than 200 °C the doubly charged ion signal disappears. At temperatures above 275 °C, a distribution of singly charged cluster ions is produced that is similar to those observed in sputtering experiments conducted using sector or quadrupole based mass spectrometers, including the increased intensities at well-known "magic numbers" that reflect the stability of structures reminiscent of the solid-state structure of NaF. As in earlier investigations, our tandem mass spectromery experiments show that the preferred dissociation channel is the loss of one or several (NaF) units and that the fragment ion intensities are influenced by the tendency to produce product ions with magic number compositions. The doubly charged cluster ions "fission" to produce singly charged fragment ions in a process analogous to that shown for sodium chloride cluster ions by Zhang and Cooks [Int. J. Mass Spectrom. 195/196 (2000) 667]. We found that the ion trap mass spectrometer is capable of performing dissociation experiments up to and including MS^8 for most cluster ions with *m/z* values greater than 401. In addition, collision-induced dissociation profiles provide information about the relative stability of inorganic cluster ions in the gas phase. For instance, we show for several cluster ions that the dissociation profiles and, in particular, the shift in activation amplitude required for dissociation, are consistent with expected differences in stability due to the adoption of magic number conformations. (Int J Mass Spectrom 207 (2001) 41–55)

Keywords: Electrospray ionization; Cluster ions; Collision-induced dissociation; Gas phase stability; Sodium fluoride

1. Introduction

Electrospray ionization (ESI) has made a remarkable impact on mass spectrometry, particularly in biological applications such as the molecular weight determination of large biopolymers (peptides, proteins, oligonucleotides, etc.) and as part of a mass spectrometry detector for separations by liquid chromatography [1–4]. The success of ESI comes from the apparent ability to "softly" transfer ionized species directly from solution to the gas phase for subsequent

* Corresponding author. E-mail: mjvansti@wsuhub.uc.twsu.edu

1387-3806/01/$20.00
PII S1387-3806(00)00454-1

mass analysis. Ion trap mass spectrometers are now commonly incorporated into commercial ESIMS instruments due in part to their low cost, small footprint and the ability to perform multiple "tandem-in-time" mass spectrometry experiments that utilize collisional activation and dissociation to gain structure and composition information about gas phase ions [5].

Although ESI has been applied successfully to problems in biological, organic, bio-organic and polymer chemistry in cases that are too numerous to list, the method has also been used to characterize species relevant to inorganic chemistry as well. Of note is the fact that ESI has been used to obtain molecular weight information for a number of inorganic anions and cations and to study metal–ligand complexes and clusters [6–11]. A principal interest of our research group is the generation of gas phase polyatomic or cluster ions and subsequent studies of their properties, including stability, reactivity, and dissociation behavior. The motivation for studies of cluster growth and the chemical and physical properties of cluster species has been provided by Castleman and Keesee [12] and by Mark and Castleman [13]. Briefly, these studies are important because cluster ions span the gap between discrete atoms or molecules and solid materials, and provide clues to the transitions between the condensed and gaseous states of matter. To date, most experimental work involving gas phase cluster ions has employed methods such as ion-induced sputtering, laser desorption/ablation, gas aggregation and expansion into vacuum to generate large polyatomic species [12,14,15]. The soft nature of ion formation, and the ability to create ions directly from solution seem to make ESI especially well suited for the generation of gas phase cluster ions from materials where sputtering or laser ablation might otherwise fail (due to the high energy input and destructive nature of the latter methods). Indeed, several recent reports have demonstrated that the formation of cluster ion series' from solutions of organic and inorganic salts is possible using ESI [16–22]. For instance, salts of the alkali metals have been used in studies designed to probe the electrospray ion formation mechanism [16,20,23,24]. More recently, Smith et al. investigated the influence of parameters such as the ionic radius, instrument settings and solution pH on the formation of cluster ions from alkali chloride and sodium salts [25]. Zhang and Cooks demonstrated that at high solution concentrations (e.g. 0.1 M) singly and, more importantly, doubly charged clusters ions can be produced and characterized from solutions of NaCl [26]. In the same report, collision-induced dissociation (CID) in an ion trap mass spectrometer was used to delineate the fragmentation pathways of the doubly charged ions and geometries for these interesting cluster species were proposed.

The purpose of this study was to further explore the performance of a commercially available ESI ion trap mass spectrometer (in this case a Finnigan LCQ-Deca™) for the generation of gas phase inorganic cluster ions. Sodium fluoride (NaF) was chosen as the test compound for this study because the previous investigations of cluster emission, intensity distributions, and dissociation of NaF and other alkali halides as studied using mass spectrometry [27–33] provide a convenient benchmark for the trap-based experiments. Of primary interest was the potential to exploit the unique features of the ion trap to investigate gas-phase ion stability, multiple dissociation steps from single precursor ions (MS^n), and gain insight into relative bond strengths using a single mass spectrometer. Our motivation here is the increasing use of ESI and ion trapping mass spectrometers to obtain a wealth of thermochemical data about gas phase ions. Examples include novel procedures to determine the thermal energy distributions of ions produced by ESI [34] and the use of "slow heating" methods in tandem mass spectrometry [35–58]. Although these advanced activation experiments were not conducted in the present study, our aim is to explore slow heating and other activation methods amenable to the LCQ instrument to probe the stability, bonding, and dissociation of inorganic and organometallic cluster species.

2. Experimental

Solutions of NaF (Aldrich Chemical, St. Louis MO) in a 50/50 mixture of methanol and deionized

H_2O were infused into a Finnigan LCQ-Deca™ (Thermoquest Corporation, San Jose, CA) using the incorporated syringe pump and a flow rate of 5 μL/min. Solution concentrations ranging from 0.1 to 100 mM were tested for optimum cluster ion generation. In general, we found that adequate cluster ion intensities in the *m/z* range 50–1500 were obtained using solutions with concentrations greater than 1 mM. This is in agreement with the study by Zhang and Cooks, in which threshold concentrations of 0.1 and 10 mM for singly and doubly charged ions, respectively, were reported. For the experimental data reported here, a solution concentration of 10 mM was used to avoid the deleterious effects of salt buildup on the ESI/capillary interface.

The atmospheric pressure ionization (API) stack settings (lens voltages, quadrupole and octapole voltage offsets, etc.) were optimized for maximum NaF cluster cation intensity at various points during the study by using the auto-tune function within the LCQ Tune program. Following the instrument tune, the spray needle voltage was maintained at +5 kV, the N_2 sheath gas flow at 35 psi, and the capillary (desolvation) temperature at a temperature appropriate for the particular experiment engaged. As shown in the following, the capillary temperature significantly influences the peak intensity distribution in the mass spectrum of NaF. During data collection, the automatic gain control on the ion trap mass spectrometer was used to set the maximum injection time.

The ion trap analyzer was operated at a pressure of $\sim 1.5 \times 10^{-5}$ Torr as measured using the remote ion gauge. Helium gas is admitted directly into the ion trap to dampen ion motion and improve trapping efficiency; He also served as the collision gas for dissociation experiments. In experiments conducted to determine the cluster fragmentation pathways by CID, the activation amplitude (proportional to collision energy) used was tuned manually until the precursor ion signal was reduced to <10% relative intensity. This corresponded to an activation amplitude of 25%–35% of the total "tickle" energy available. For all CID experiments an isolation width of 2.5–3.5 *m/z* units, an activation *Q* setting (rf excitation frequency, as labeled by Thermoquest in the LCQ operation software) of 0.25, and an activation time of 30 ms were used. The isolation width, centered on the centroid of the precursor ion peak, was adjusted based upon the intensity of the cluster: lower intensity peaks required wider activation widths. During CID experiments designed to measure relative gas phase stability, in which the ESI source was operated for extended periods of time, the Orthogonal Sampling Adapter™ (OSA) was used to further protect the heated capillary from excessive salt build-up. The use of the OSA did not effect the ion intensity distributions, CID patterns or stability measurements.

To obtain collision-dissociation profiles or breakdown curves (the decrease in precursor ion intensity as a function of collision energy) for various cluster ions, the activation amplitude was increased by 1%–2% increments of the maximum amplitude through a range of 10%–30%. The range used in these experiments was sufficient to produce quantitative data progressing from 100% precursor ion intensity to nearly complete conversion to product ions (<5% precursor ion intensity). Relative precursor and product ion intensities were collected by summing 20 scans for each collision energy. The precursor and product ion intensities were then converted to a percentage of the total summed ion current.

3. Results and discussion

3.1. Mass spectra and influence of operating parameters

Fig. 1 shows the positive ESI mass spectrum of NaF, highlighting the *m/z* range 100–900 [Fig. 1(a)] and *m/z* 900–1800 [Fig. 1(b)]. The mass assignments for the majority of the prominent ions observed were consistent with the formation of a cluster series represented by the formula $(NaF)_nNa^+$. The spectra shown in Fig. 1 were produced at a capillary temperature of 275 °C. At this temperature, and tuning the API stack settings using either the cluster ions at *m/z* 359 or 569, the value of *n* ranged from 1 to 46. Additional minor peaks, not labeled in Fig. 1, were consistent with the addition of (NaOH) units to

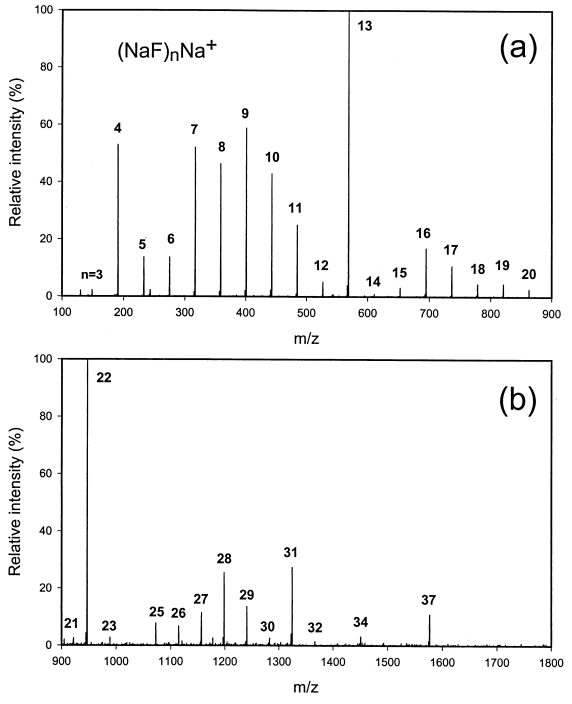

Fig. 1. Positive electrospray ionization ion trap mass spectrua of NaF, showing the $(NaF)_nNa^+$ cluster ions observed in the *m/z* range (a) 100–900 and (b) 900–1,800. The numeral located above each major peak corresponds to the number of (NaF) units within each cluster ion.

$(NaF)_nNa^+$ "core" ions including and those larger than *m/z* 149 [$(NaF)_3Na^+$]. The apparently mixed fluoride/hydroxide cluster ions were present at the start of each experimental run, and their intensity relative to the $(NaF)_nNa^+$ series increased as prepared solutions were allowed to sit for a period of days. Negative cluster ions, of the form $(NaF)_nF^-$, were weaker in intensity than the positive cluster ions, and were more difficult to generate reproducibly. We therefore continued the investigation by concentrating on the positive cluster ions only.

Hao and co-workers have reported that solution concentration, solvent choice, desolvation temperature (capillary temperature in LCQ instruments), and infusion flow rate do not significantly alter the ion intensities within ESI mass spectra of, for instance, sodium salts of acetate, chloride, and nitrate [25]. Because our prime concern is the cluster ion distribution and not simply the overall ion intensity, we thoroughly investigated the influence of various LCQ-Deca™ API stack operating parameters on the NaF cluster ion intensities observed following ESI. These parameters included the N_2 sheath gas flow rate, capillary voltage, capillary (desolvation) temperature, spray voltage, and tube lens offset voltage; each chosen based on the manufacturers recommendations of those that were most likely to influence ion intensities. Of these parameters, only the capillary temperature significantly altered the cluster ion intensity distribution, and because of the importance of this influence to the interpretation of cluster ion distributions, we discuss our observations here in detail. Fig. 2 shows four mass spectra, highlighting the *m/z* range 50–1500, obtained using capillary temperatures ranging from 100 to 250 °C. At low capillary temperatures (i.e. 100–120 °C) the mass spectrum includes several singly charged and doubly charged $(NaF)_n$ cluster species in addition to a series of peaks with *m/z* values characteristic of Na^+ ions with one or several attached H_2O and MeOH molecules. The doubly charged species adopt the formula $(NaF)_mNa_2^{+2}$, and clusters with even values of *m* have *m/z* ratios that overlap singly charged ions within the $(NaF)_nNa^+$ cluster series. At a capillary temperature of 150 °C, the low mass Na/H_2O/methanol peaks decreased in intensity, as did several of the doubly charged NaF cluster ions, and the peak intensity distribution displayed maxima at *m/z* 275, 401, 569, and 947. At a capillary temperature of 200 °C, the doubly charged clusters were no longer apparent, and the intensities of the peaks at *m/z* 233, 275, 359, 401, and 443 showed marked decreases compared to the relative intensity observed at lower capillary temperatures. These observations indicate that at moderate capillary temperatures (100–120 °C), complete desolvation does not occur, leading to the detection of Na cations with attached solvent molecules. At capillary temperatures between 130 and 175 °C, less stable cluster ions, either singly or doubly charged, apparently proceed through the desolvation step and transfer to the mass analyzer intact. Within the ion trap, "cooling" collisions with the He bath gas may assist the survival and detection of these ions further. At higher capillary or desolvation temperatures, such as those above 200 °C, decomposition of

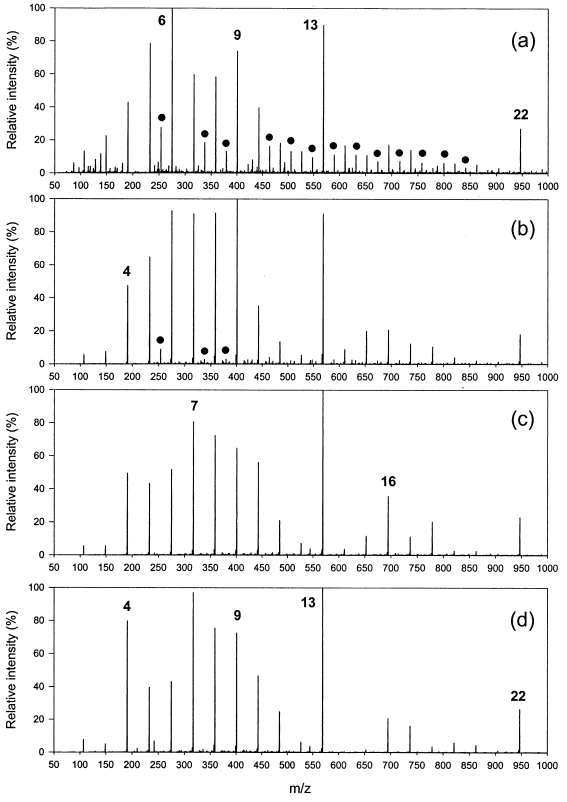

Fig. 2. Positive electrospray ionization ion trap mass spectra, *m/z* range 50–650, of NaF at four different capillary temperatures (a) 100, (b) 150, (c) 200, and (d) 250 °C. All other experimental conditions were held constant. The spectra demonstrate the significant influence of the capillary temperature, used to desolvate ions en route to the skimmer region, on the peak intensity distribution. Filled circles above the peaks in (a) and (b) mark the presence of odd-numbered doubly charged species.

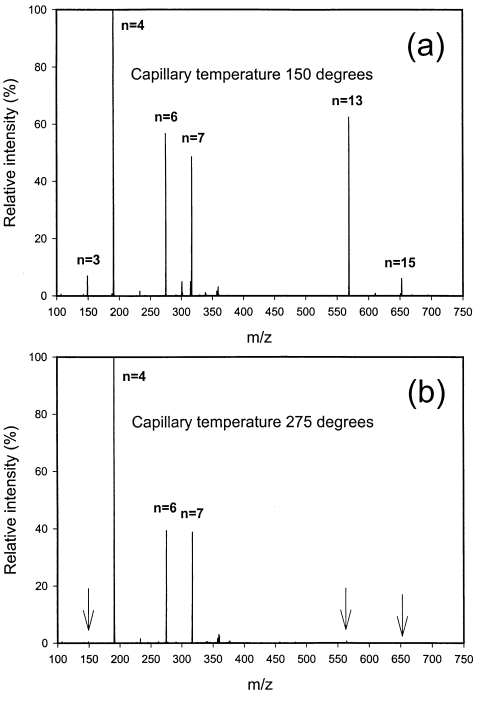

Fig. 3. Collision-induced dissociation spectra for the peak at *m/z* 359 using capillary temperatures of (a) 120 and (b) 275 °C. The arrows in (b) indicate the absence of fragment ions generated from the dissociation of the doubly charged $(NaF)_{16}Na_2^{2+}$ cluster.

less stable cluster ions occurs and the ESI ion trap mass spectrum is biased towards the more stable cluster ion species. These observations are very much in line with the results reported by Busman et al., who demonstrated that the heated capillary in an ESI interface, in addition to the usual application to desolvate ions, can be used as a "thermal reaction vessel" to study the thermal dissociation of ions [59]. Zhang and Cooks, in their study of the dissociation of doubly charged sodium chloride cluster ions, noted that the capillary temperature in an LCQ instrument influences the overall intensities of doubly and singly charged sodium chloride cluster ions in a fashion consistent with the assumption that "more energetic conditions decrease cluster stability" [26]. The decrease in intensity of the peaks at *m/z* 233, 275, 359, 401, and 443, and several higher mass ions, may be due to the loss of the fraction of the population within each peak attributable to doubly charged ions. For instance, the peak at *m/z* 359 corresponds to the singly charged cluster ion $(NaF)_8Na^+$ and the doubly charged cluster ion $(NaF)_{16}Na_2^{+2}$. Fig. 3 shows the CID spectrum collected for the *m/z* 359 ion at capillary temperatures of 120 °C [Fig. 3(a)] and 275 °C [Fig. 3(b)]. At higher capillary temperatures, the fragment ions resulting from the dissociation of the doubly charged ion are noticeably absent, indicating that at a temperature of 275 °C the *m/z* 359 peak is composed of singly charged $(NaF)_8Na^+$ ions. It is plausible that several of the nonmagic number singly charged cluster ions are also unstable to thermal dissociation to varying degrees and decreases in peak

intensity also reflect the thermal decomposition of these species. We assume, therefore, that the modification of the peak intensity distribution as a function of capillary temperature is a composite of (1) the thermal dissociation and loss of doubly charged cluster ions, and (2) the decomposition of less stable singly charged cluster ions.

At 275 °C the ion intensity distribution included maxima at the several magic numbers characteristic of alkali halide cluster species. For instance, the cluster ions at n=4 (*m/z* 191), 7 (*m/z* 317), 13 (*m/z* 569), and 22 (*m/z* 947) are more prominent that those either one (NaF) unit larger or smaller. In the case of the $n = 13$ and 22 cluster ions, the intensity is significantly higher than, for instance, the $n = 12$, 14, and 21 cluster ions. Magic numbers were also observed at $n = 28$, 31, and 37. The identification of these peaks as singly charged NaF cluster ions is plausible in light of the observation that doubly charged species are thermally dissociated at high capillary temperatures. The observation of magic numbers in the cluster ion intensity distribution are not unique to this study: they have been reported in earlier studies involving, for example, sputtering of alkali halides [27,29,60], ESI mass spectrometry of sodium salts [25] and positive ion emission from megaelectron volt ion impacts on $NaBF_4$ [33]. Calculations of the energies for different cluster geometries have shown that species with magic number compositions have higher stability owing to the adoption of gas phase configurations that are reminiscent of the solid-state structure of the alkali halides [61]. For instance, the $n = 4$, 7, 13, and 22 cluster ions may form $3 \times 3 \times 1$, $3 \times 5 \times 1$, $3 \times 3 \times 3$ and $3 \times 5 \times 3$ lattice structures, respectively. The close-packed, cuboidal structures in the gas phase have been confirmed using ion mobility/mass spectrometry measurements of $(NaCl)_nNa^+$ cluster ion conformation [62]. The experiments also included an important demonstration of temperature dependent changes in structure for cluster ions of a given *m/z* value.

Magic number values for the doubly charged cluster ions were more difficult to determine. First, neither Na nor F have multiple stable isotopes, prohibiting the determination of charge state by peak spacing, and hence the abundance of $(NaF)_mNa_2^{2+}$ ions within peaks that also contain $(NaF)_nNa^+$ species. For instance, in their study Zhang and Cooks used the isotopomer distribution due to ^{35}Cl and ^{37}Cl to determine the abundance of (doubly charged) $(NaCl)_nNa_2^{2+}$ species. Second, we found, as did Zhang and Cooks, that the relative intensities of the doubly charged ions are extremely sensitive to the capillary temperature used to desolvate ions. The determination of magic numbers for the $(NaF)_nNa^+$ cluster distribution was facilitated by the ability to raise the capillary temperature to dissociate thermally labile clusters ions. This accentuated the magic number species; those with higher intrinsic stability due to the adoption of square planar and cuboidal geometric arrangements. An approach using the capillary temperature to identify and accentuate the magic numbered doubly charged species was hindered by the fact that even modest increases in temperature (up to ~150 °C) significantly reduced and eventually eliminated the doubly charged ion signal. At the lowest capillary temperature used here, 100 °C, the intensity distribution for the doubly charged species could be estimated using the following approach. For the peaks at which singly and doubly charged species overlapped the decrease in peak intensity with increasing capillary temperature was used as a relative measure of the doubly charged ion fraction present, with the caveat that the loss in intensity due to the dissociation of singly charged ions undoubtedly introduced error into this estimate. For instance, the peak at *m/z* 275, which contains singly charged $(NaF)_6Na^+$ and doubly charged $(NaF)_{12}Na_2^{2+}$, decreased in intensity by ~30% when the capillary temperature was raised from 100 to 200 °C, thus providing an upper limit to the contribution to the peak abundance by the doubly charged species. The odd numbered doubly charged species (odd values of m) could be identified unambiguously and their intensities were recorded directly. Estimating the relative abundances within the of the doubly charged peak distribution using this approach, we found that the $(NaF)_mNa_2^{2+}$ series exhibited magic numbers at values similar to those reported for $(NaCl)_mNa_2^{2+}$ [26], including the species at $m = 11$, 12, 17, 20, 21, 30, 34, and 36.

3.2. Collision-induced dissociation of singly and doubly charged cluster ions

As noted earlier, the object of this study was to probe the general utility of ESI and the LCQ-Deca™ for studying the formation of extended series of gas phase cluster ions, and in particular to gain insight into general patterns in stability and bonding. The "trapping" mass analyzers such as the quadrupole ion trap and ion cyclotron resonance mass spectrometers are unique in allowing tandem-in-time tandem mass spectrometry experiments to be conducted using a single mass analyzer [5]. With sufficient precursor ion signal and CID efficiency, the LCQ-Deca™ permits MS^n measurements with $1<n<10$. We explored the effectiveness of the ion trap for CID studies of the NaF cluster ions in the tandem mass spectrometry and MS^n modes. At a capillary temperature of 275 °C, each singly charged cluster ion from $n = 2$ to 46 could be isolated, collisionally activated and dissociated into fragment ions. The tandem mass spectrometry results for the $(NaF)_nNa^+$ ions are listed in Table 1. To produce CID spectra from the singly charged ions, activation amplitudes of 25%–35% and an activation Q [radio frequency (rf)] setting of 0.25 were employed. With this set of activation parameters, the relative intensities of each fragment ion for each precursor were as shown in parenthesis in Table 1. For cluster ions with multiple dissociation pathways, we observed that the relative intensities of the fragment ions were sensitive to the activation amplitude used, with high amplitudes causing increased intensities of the lower mass fragment ions. A fragment ion, assumed to be Na^+, resulting from the CID of the $n = 1$ cluster ion at m/z 65 could not be trapped and detected. In general, we find it difficult to trap and detect ions below m/z 25 despite setting an injection radio frequency sufficient for a low-end cutoff of m/z 15.

Consistent with several earlier studies of the dissociation of alkali halide cluster ions, the principal dissociation pathway involves the emission of one or more neutral (NaF) units [25,26,28,33]. In several cases, such as for the $n = 11$–13 and the $n = 17$ and 18 cluster ions, the loss of two NaF units was more probable than the loss of a single unit. We observed also that a preferred dissociation channel is often one that leads to a fragment ion with a magic number cluster composition. This was demonstrated, for example, by the preferential dissociation of the $n = 7$–9

Table 1

Precursor ion, n	Fragment ions, n
2	1
3	2
4	3 (100), 2 (45), 1 (34)
5	3
6	4
7	6 (7), 5 (30), 4 (100)
8	7 (50), 6 (50), 4 (100)
9	8 (30), 7 (100), 6 (1), 5 (1), 4 (1)
10	9 (100), 8 (23), 7 (13), 6 (3), 4 (17)
11	10 (22), 9 (100), 8 (5), 7 (4)
12	11 (35), 10 (100), 8 (11), 8 (6)
13	12 (10), 11 (100), 10 (9), 9 (9), 7 (1)
14	13
15	13
16	13
17	16 (50), 13 (100)
18	17 (50), 16 (100)
19	17 (100), 16 (8), 15 (22)
20	19 (100), 18 (23), 17 (98), 16 (43), 13 (20)
21	20 (45), 19 (100), 18 (4), 17 (30), 13 (7)
22	21 (20), 20 (100), 19 (40), 17 (20), 16 (8), 13 (6)
23	22 (100), 21 (2), 20 (4)
24	22
25	22
26	25 (15), 22 (100)
27	26 (34), 25 (100), 22 (57)
28	27 (100), 26 (65), 25 (23), 24 (60)
29	28 (100), 27 (40), 26 (5), 25 (5), 22 (3)
30	29 (60), 28 (100), 27 (5), 26 (3), 25 (3), 22 (3)
31	29 (100), 28 (40), 27 (15), 26 (3), 25 (3), 22 (3)
32	31 (100), 30 (20), 29 (3), 28 (3)
33	32 (30), 31 (100), 30 (3), 28 (3)
34	33 (10), 32 (10), 31 (100), 29 (5)
35	34 (100), 33 (10), 31 (15)
36	35 (40), 34 (100), 33 (5), 31 (5)
37	36 (20), 35 (40), 34 (100), 31 (10)
38	37 (100), 36 (20), 35 (10), 34 (15)
39	38 (10), 37 (100), 36 (2), 35 (2)
40	39 (10), 38 (10), 37 (100)
41	40 (20), 39 (20), 37 (100)
42	41 (10), 40 (25), 39 (10), 37 (100)
43	42 (100), 41 (20), 40 (20), 39 (10), 37 (37)
44	43 (100), 42 (80), 41 (5), 40 (10), 37 (15)
45	44 (60), 43 (100), 42 (20), 37 (5)
46	45 (60), 44 (100), 43 (60), 37 (6)

precursor ions into the $n = 4$ fragment ion; the $n = 17$ precursor ion into the $n = 13$ fragment ion; the $n = 24$–28 precursor ions into the $n = 22$ fragment ion and the $n = 38$–42 precursor ions into the $n = 37$ fragment ion. The results from the ESI CID experiments for the cluster ions from $n = 2$–10 compare well to those obtained using a reflectron time-of-flight analyzer and the ion–neutral correlation method to probe the metastable dissociation pathways for $(NaF)_nNa^+$ clusters generated from megaelectron volt ion impacts on $NaBF_4$ [33]. For a given precursor ion, the CID experiments showed one or more additional fragmentation pathways, however, which can be rationalized by the fact that the energy input by collisional activation may provide access to channels not apparent when probing metastable dissociation reactions. Because ions with *m/z* ratios lower than 50 were below the low mass range cutoff of the trap in the CID experiments, we cannot rule out the loss of Na^+ as a dissociation channel for the higher mass cluster ions. We note, however, that such a channel was not observed in the reflectron TOF studies [33], in which ions below *m/z* 50 were detected with high efficiency.

At a capillary temperature of 120 °C, the CID patterns of the doubly charged cluster ions could also be studied. The doubly charged ions with odd values of m could be unambiguously identified and isolated and their CID spectra were recorded directly. For cases in which singly and doubly charged species overlapped to produce a single peak, the CID patterns at 120 and 275 °C (i.e. above the temperature at which doubly charged ions are thermally dissociated) were compared to identify those fragment ions attributable to the dissociation of the doubly charged ions. By way of direct identification and comparative dissociation at two capillary temperatures, we concluded that the series of doubly charged ions, $(NaF)_mNa_2^{2+}$, extended from $m = 10$–48. Fig. 4 shows the CID spectra obtained for the doubly charged species $(NaF)_{15}Na_2^{+2}$ and $(NaF)_{21}Na_2^{+2}$, and an example of the identification of doubly charged ions by fragmentation at two capillary temperatures was provided in Fig. 3. The results of the CID experiments involving the doubly charged clusters are summarized in Table 2. As with the singly charged ions, and activation amplitude of

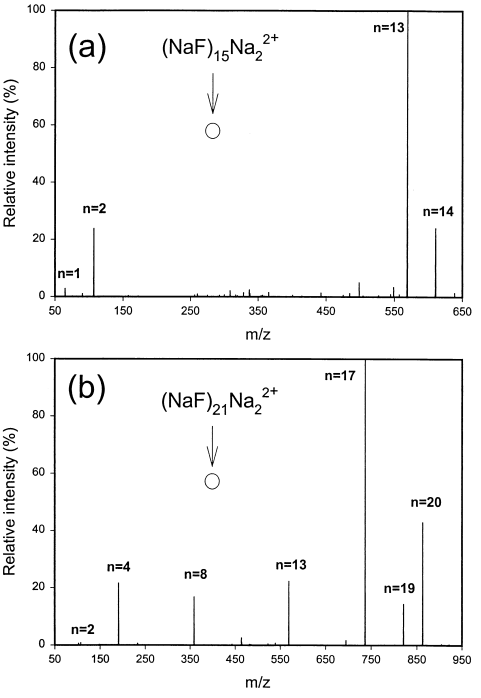

Fig. 4. Collision-induced dissociation spectra for the doubly charged ions (a) $(NaF)_{15}Na_2^{2+}$ and (b) $(NaF)_{21}Na_2^{2+}$. The CID spectra were collected using a capillary temperature of 120 °C.

30% and an activation *Q* setting of .25 were used to produce the data in Table 2. We observed that the CID patterns for the doubly charged peaks were sensitive to the choice of activation amplitude as well as the radio frequency excitation frequency. In general, the kinetic energy of the collision events is proportional to the square of the activation *Q* value [63]. Adjusting the activation *Q* parameter to lower values (~0.15–0.2 compared to the default value of 0.25) often produced CID patterns that included only the fragment ions from the even numbered doubly charged ions when peaks known to also contain a singly charged $(NaF)_nNa^+$ ion were isolated and dissociated. For example, Fig. 5 shows the CID spectra for the peak at *m/z*359, collected using different values of activation *Q* and activation amplitude. Fig. 5(a) was obtained using a *Q* setting of 0.25, an activation amplitude of 30% and an activation time of 300 ms. The spectrum in Fig. 5(b) was collected using an activation *Q* value of 0.15, an activation amplitude of

Table 2

Precursor ion, *m*	Fragment ions, *n*
10	9 (100), 7 (5), 6 (2), 10 (100), 1 (26)
11	10 (100), 1 (26)
12	11 (100), 10 (16), 8 (30)
14	13 (100), 12 (5), 11 (5), 10 (10)
15	14 (25), 13 (100), 2 (25), 1 (4)
16	15 (15), 13 (100), 3 (15)
17	16 (30), 13 (100), 4 (35), 1 (2)
18	17 (100), 16 (5), 14 (5), 6 (3), 13 (15)
19	18 (55), 17 (100), 16 (50), 15 (15), 13 (10), 6 (80), 4 (5) 3 (10), 2 (20)
20	19 (100), 16 (30), 13 (10)
21	20 (45), 19 (15), 17 (100), 13 (25), 8 (20), 4 (25)
22	22 (100), 20 (5), 13 (5)
23	22
24	24 (10), 23 (8), 22 (100), 3 (5)
25	24 (10), 23 (8), 22 (100), 3 (5)
26	25 (30), 22 (100), 20 (5)
27	26 (100), 26 (20), 23 (30), 22 (60), 13 (10), 5 (20), 4 (10) 3 (1)
28	27 (100), 22 (10)
29	28
30	29 (100), 28 (5)
31	31 (10), 30 (100), 29 (50), 28 (15), 27 (2), 15 (10)
32	31 (100), 28 (5), 22 (3)
33	32 (25), 31 (100), 29 (35), 16 (30)
34	33 (100), 32 (15), 31 (80), 30 (15), 29 (20), 28 (20), 27 (15), 26 (5), 25 (5), 22 (20), 20 (10)
35	34
36	35 (100), 34 (20), 22 (5)
37	37 (100), 36 (35), 35 (10), 34 (10), 31 (5), 18 (85)
38	37 (20), 34 (5), 25 (5)
39	38 (100), 37 (10)
40	39 (100), 37 (10)
41	40 (10), 37 (100)
42	41 (60), 40 (10), 39 (15), 37 (100)
43	42 (100), 41 (10), 40 (4), 39 (15), 37 (60), 37 (100)
44	43
45	44 (100), 43 (50), 42 (10), 37 (12), 22 (60), 21 (15) 19 (20), m = 43 (25)
46	45 (50), 44 (45), 43 (40), 42 (10), 37 (20), 34 (6) m = 45 (100)

15% and an activation time of 300 ms. The low radio frequency and amplitude settings apparently allow "gentle" collisional activation such that the CID pattern exhibits only the fragment ions from the doubly charged species. This conclusion is based on the observation of only those fragment ions consistent

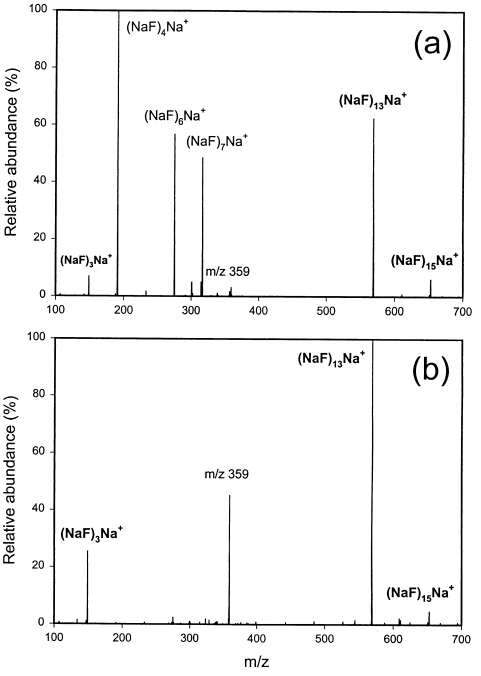

Fig. 5. Collision-induced dissociation spectra produced from the peak at *m/z* 359 [$(NaF)_8Na^+$ and $(NaF)_{16}Na_2^{2+}$] collected using the following activation parameters: (a) radio frequency (activation Q) = 0.25, activation amplitude = 30% and activation time = 300 ms and (b) radio frequency = 0.15, activation amplitude 15% and activation time = 300 ms. The fragment ion peaks labeled with boldface text indicate those attributable to the dissociation of the doubly charged species.

with the fission of the doubly charged species and the lack of those due to the loss of one or several (NaF) units from the singly charged peak [for instance, compare Fig. 5(a) to 3(b)]. Similar results were observed for all peaks in which singly and doubly charged ions overlapped at the same *m/z*value.

When probing the dissociation of $(NaCl)_mNa_2^+$ cluster ions, m = 11–67, Zhang and Cooks reported that a dominant dissociation mechanism for smaller doubly charged species is a fission process to produce singly charged fragment ions, with a shift for higher mass clusters to a mechanism whereby the ions dissociate to produce doubly charged fragment ions [26]. Overall, our observations for the doubly charged NaF cluster ions were similar but with two notable differences. First, the smallest doubly charged NaF cluster ion detected was $(NaF)_{10}Na_2^{2+}$, one (NaF) unit

smaller than the analogous ion in the NaCl cluster series. Second, in the case of NaF the production of doubly charged fragment ions following CID of the doubly charged precursor ions was less prevalent than reported for NaCl, and the onset of this mode of fragmentation was not observed until the cluster ion at m=43. The onset of doubly charged fragment ion production during CID of the NaCl cluster ions was m=27.

Zhang and Cooks have eloquently proposed geometrical arrangements for the doubly charged (NaCl) ions that include combination blocks, merged blocks and single-point defect structures [26]. The fluoride and chloride ions have radii of 133 and 181 pm, respectively. Of the two, the fluoride ionic radius is closer to that of Na^+ (102 pm), and we therefore expect stronger bonding within the clusters between Na and F than Na and Cl. Indeed, this hypothesis is supported by the difference in calculated lattice energy (the energy required to separate two ions within a crystal to infinite distances) for NaF and NaCl crystals (910 and 769 kJ/mol, respectively). Because both NaF and NaCl assume rock-salt crystal structures, the doubly charged (NaF) cluster ions likely adopt configurations similar to those proposed for NaCl by Zhang and Cooks. Based on the differences in ionic radius, one might expect the NaF species to adopt more tightly packed structures.

Fig. 6 shows the tandem mass spectrometry, MS^3, MS^4, and MS^5 spectra collected using the n = 13 cluster ion at *m/z* 569 and a capillary temperature of 275 °C. The tandem mass spectrometry spectrum includes a prominent fragment ion at *m/z* 485 (n = 11) and weaker intensity fragments at *m/z* 401, 443, and 527, corresponding to the cluster ions at n = 9, 10, and 12, respectively. Isolation and dissociation of the *m/z* 485 fragment ion (MS^3) in turn produces product ions at *m/z* 317, 359, 401, and 443, corresponding to the n = 7, 8, 9, and 10 cluster ions, respectively. Further CID of the most abundant fragment ions after each step (MS^4 and MS^5, Fig. 6(c) and (d) ultimately produced the n = 4, 5, and 6 cluster ions. In several cases for cluster ions of high values of n, it was possible to perform CID measurement equivalent to MS^8, demonstrating the potential for performing extensive composition and structurally informative dissociation steps from single precursor ions within a suite of homologous cluster species.

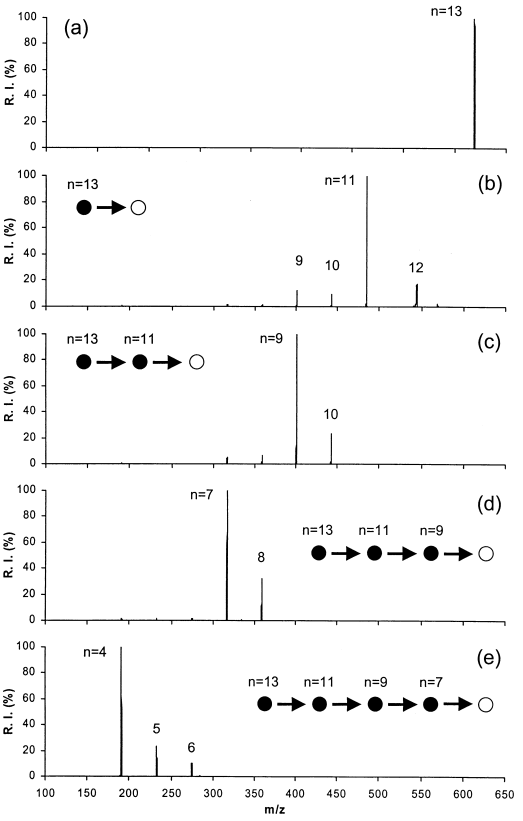

Fig. 6. MS^n spectra beginning with the isolation and CID of the $(NaF)_{13}Na^+$ cluster species: (a) isolation of the n = 13 ion with no activation energy applied to affect CID, (b) tandem mass spectrometry spectrum obtained for the n = 13 ions using 30% activation amplitude, (c) MS^3 of n = 11 fragment ion, (d) MS^4 of n = 9 fragment ion, and (e) MS^5 of 7 fragment ion. The CID spectra were collected using a capillary temperature of 275 °C.

3.3. Collision-induced dissociation profiles

The use of the ion trap mass analyzer to provide insight into the relative stabilities and bonding of ions, particularly for noncovalently bound complexes [64,65] has recently been demonstrated. Using an approach similar to that reported by Gross and coworkers [64], we examined the dissociation behavior of several NaF cluster ions in detail, focusing on the

cluster ions with magic number compositions and those that immediately precede each magic number. Gas-phase stability can be studied by subjecting an ion to increasing activation amplitude (collision energy) in the ion trap and monitoring the relative abundance of precursor and product ions as a function of the relative collision energy. Theoretical investigations of alkali halide cluster structures predict that the magic number intensity anomalies arise due to the adoption of cube and column-like structures, similar to the rock salt crystal structure, that have lower energies than ring-shaped or linear structures [61]. Because of the stability due to geometrical arrangement, our premise was that the magic number ions should show dissociation profiles (CID breakdown curves) that are clearly distinct from non-magic number cluster ions, i.e. shifted in such a way as to reveal tighter bonding, and provide an important test to the sensitivity of the dissociation profile to changes in inorganic or ionic cluster ion stability.

The dissociation profiles, obtained by monitoring ion intensity versus activation amplitude, are shown for several pairs of NaF cluster ions in Figs. 7 and 8. To ensure that the dissociation profiles were being collected for only the singly charged, $(NaF)_nNa^+$ cluster ions, a capillary temperature of 275 °C was used. The lack of adjacent, purely doubly charged ion peaks in the spectrum at lower capillary temperatures prohibited the comparison of dissociation profiles for those species.

Fig. 7 shows the characteristic S-shaped profiles of the decrease in intensity for (1) the $n = 6$ cluster and the magic number cluster $n = 7$ and (2) the $n = 12$ cluster and the magic number cluster at $n = 13$. Fig. 8 shows the profiles for $n = 21$ and the magic number $n = 22$ [Fig. 8(a)] and those for the nonmagic number cluster ions at $n = 8$ and $n = 9$ [Fig. 8(b)]. The cluster ions at $n = 8$ and 9 were included as a control: the difference in bond strength or stability between the adjacent, nonmagic number cluster ions was expected to be significantly less than the difference between the magic number species and those one NaF unit smaller. In both Figs. 7 and 8, the relative increases in fragment ion intensity are also shown for the sake of comparison. In cases where precursor ions

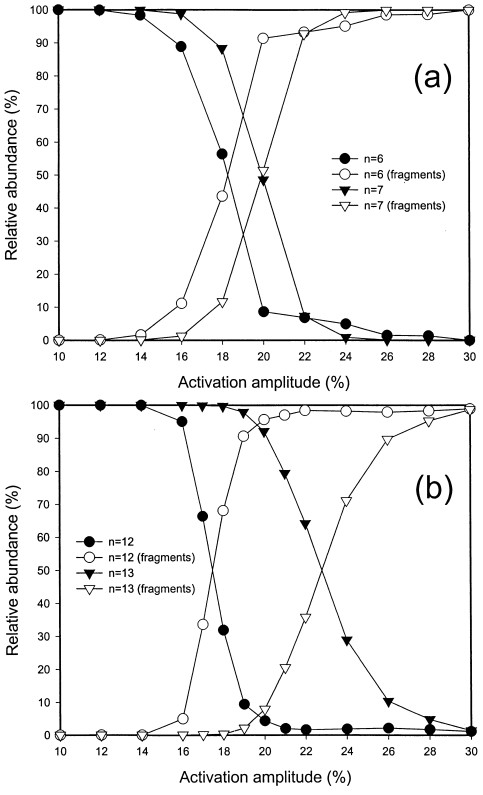

Fig. 7. CID dissociation profiles for: (a) $n = 6$ and $n = 7$ and (b) $n=12$ and $n=13$ cluster ions. For comparison, the increases in total fragment ion abundance (identified with the letter F in the legend) are also shown. The methodology for the production of dissociation profiles is provided in the experimental section.

exhibited multiple dissociation pathways, the relative intensities of the fragment ions were summed to produce the relative fragment ion intensity. It is clear from the plots in Figs. 7(a) and (b), and 8(a) that there are significant differences in the dissociation profiles, with a pronounced shift to higher activation amplitude (and hence collision energy) required to dissociate each magic number cluster ion relative to the cluster ion one NaF unit smaller. The exception is for the pair $n = 8$ and $n = 9$, which show very similar profiles. It is interesting to note the fact that the largest shift in dissociation profile position, and therefore collision energy required for dissociation, occurs when comparing the $n = 12$ and $n = 13$ cluster ions. The latter ion is in most cases the most abundance cluster ion observed in the ESI mass spectrum of NaF.

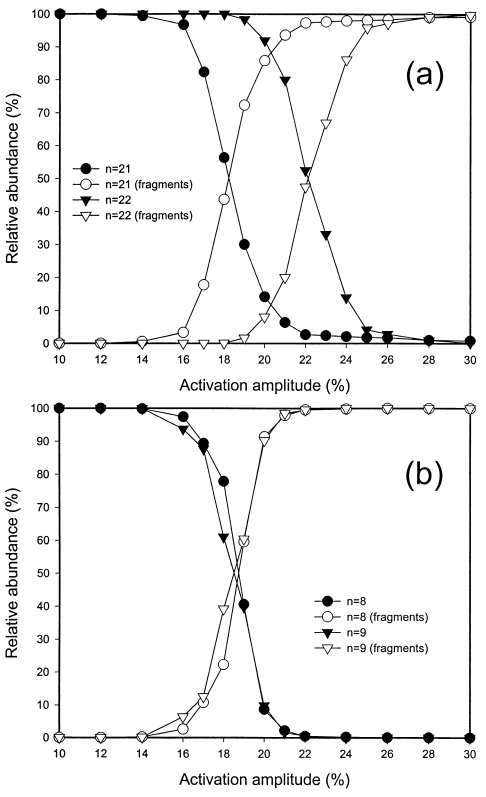

Fig. 8. CID dissociation profiles for: (a) $n = 21$ and $n = 22$ and (b) $n = 8$ and $n = 9$ cluster ions. For comparison, the increases in total fragment ion abundance (labeled with the letter F in the legend) are also shown.

CID spectra and fragment ion intensities are influenced by the mass and complexity (or degrees of freedom) of the precursor ion and by kinetic shifts (i.e. the energy above the threshold energy for dissociation required produce fragmentation observable within the time-window accessed by the mass spectrometer). The maximum collision energy converted to internal energy, in general, is proportional to the relative collision energy and inversely proportional to precursor ion mass. The cluster ions compared in each plot shown in Figs. 7 and 8 differ by only 42 mass units (one fluorine and one sodium atom), and neither this mass difference nor possible kinetic shifts are expected to prohibit the use of dissociation profiles to compare the relative stability of adjacent cluster species. Indeed, the clear differences demonstrated by

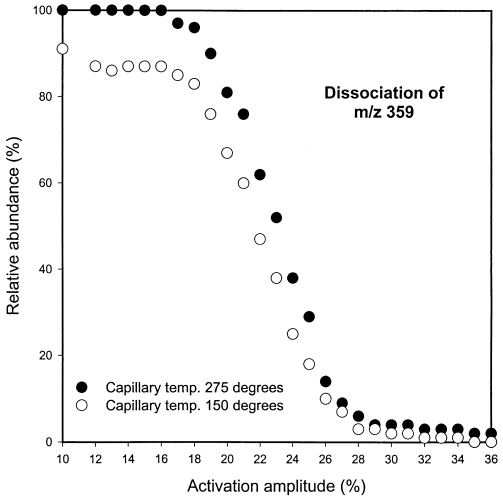

Fig. 9. CID dissociation profiles for the peak at *m/z* 359 collected at capillary temperatures of 120 °C (open circle) and 275 °C (closed circle). The corresponding plots of increase in fragment ion intensities have been omitted for the sake of clarity.

the pairs $n = 12/n = 13$ and $n = 8/n = 9$ demonstrates that the dissociation profile is influenced more by the intrinsic stability of the ion. The slight shift to higher collision energies in the dissociation profile for the $n = 8$ ion relative to the $n = 9$ species is consistent with slightly tighter bonding in the smaller cluster ion. Neglecting "magic number cases," the bonding in a cluster ion within a homologous series, in general, is expected to decrease with increasing size [33,66,67].

Dissociation profiles were also collected for the same precursor ion at varying capillary temperatures. This was done to probe the sensitivity of the profile to the presence of doubly charged species or unstable (perhaps with higher internal energy after formation and desolvation) singly charged ions within a particular peak in the mass spectrum. For instance, as noted earlier the peak observed at *m/z* 359, when examined at low capillary temperature, was composed of (singly charged) $(NaF)_8Na^+$ and (doubly charged) $(NaF)_{16}Na_2^{+2}$. Fig. 9 compares the dissociation profile for the *m/z* 359 peak at capillary temperatures of 120 and 275 °C. The increase in fragment ion intensity was not included in Fig. 8 for the sake of clarity. The dissociation profile for the peak collected at the lower temperature is influ-

enced by the appearance of a singly charged fragment ion from the metastable dissociation of the doubly charged ion. This leads to a decrease in the initial intensity of the precursor ion (sum of doubly and singly charged ions) at low activation amplitudes. A significant difference in the shapes of the two profiles was observed within the activation amplitudes range from 17% to 27%, and this difference is likely due to the fact that the doubly charged species within the peak are dissociated at lower relative collision energies. The presence of doubly charged ions with lower stability would lead to greater loss of precursor ion intensity at low activation amplitudes, particularly when the dissociation profile collected at a low capillary temperature is compared to the CID of the same ion at the higher capillary temperature.

4. Conclusions

The data presented here for NaF, when combined with that reported by Zhang and Cooks for NaCl, provide convincing evidence that commercially available ESI ion trap mass spectrometry instrumentation is well suited for the study of gas phase cluster ions. We add to previous studies by pointing out that while ESI produced a series of singly charged and doubly charged cluster ions from NaF, the intensity distribution of these ions was sensitive to the capillary (desolvation) temperature. High capillary temperatures, in the case of NaF those above 200 °C, cause the decomposition of unstable cluster ions and increase the relative prominence of more stable, magic number species. This indicates that a range of capillary temperatures should be examined before drawing conclusions about the cluster ion intensity distributions produced by ESI (as opposed to the distribution following modification by processes operative during desolvation and transfer of ions to the mass analyzer) and the magic numbers observed using the ion trap analyzer. Discussion of the capillary temperature and its influence on the ion intensity distribution is relevant to Finnigan ESI interfaces. It is likely, however, that similar effects will be observed in ESI interfaces that employ other means to evaporate solvent molecules prior to transfer through the skimmer region and to the mass analyzer. March and co-workers have reported, for instance, that the cone voltage setting on the Quattro LC TSQ (Micromass, Manchester UK) ESI instrument significantly influences the ion intensity distribution [25]. We note also that the intensity distributions of cluster ions observed in MS, in general, are often very sensitive to the choice of mass analyzer as well.

In addition, we found that the LCQ-Deca™ provides the opportunity to perform important CID tendem mass spectromety and MS^n experiments with inorganic cluster ions, and by varying the relative collision energy of isolated ions, useful information about the relative stabilities and bonding of cluster ions can be obtained. Gross and co-workers have stated previously that the ion trap method for probing intrinsic ion stability provides only a qualitative assessment, and can not supply absolute values in terms of the energetics of bonding because of experimental uncertainties with respect to the kinetic energy during the collision events in ion traps [64]. Our experiments show that the dissociation profiles can reveal relative differences in stability for adjacent species within a cluster ion series. Future work will involve the development of experimental protocols designed to compare stability across an entire cluster distribution.

Acknowledgements

Generous financial support for this work from the Wichita State University College of Liberal Arts and Sciences and the National Science Foundation through the EPSCoR program (EPS-9874932) is gratefully acknowledged. The authors also thank Mark Brock and Larry Burchfield of the Thermoquest Corporation for their assistance with the installation and operation of the ESI ion trap instrument.

References

[1] S.J. Gaskell, J. Mass Spectrom. 32 (1997) 677.
[2] C.M. Whitehouse, R.N. Dreyer, M. Yamashita, J.B. Fenn, Anal. Chem. 64 (1985) 675.
[3] J.B. Fenn, M. Mann, C.K. Meng, S.F. Wong, C.M. Whitehouse, Science 246 (1989) 64.
[4] J.B. Fenn, M. Mann, C.-K. Meng, S.-F. Wong, C.M. Whitehouse, Mass Spectrom. Rev. 9 (1990) 37.
[5] R.E. March, J. Mass Spectrom. 32 (1997) 351.
[6] R. Colton, A. D'Agostino, J.C. Traeger, Mass Spectrom. Rev. 14 (1995) 79.
[7] P J. Dyson, B.F. G. Johnson, J.S. McIndoe, P.R.R. Langridge-Smith, Inorg. Chem. 39 (2000) 2430.
[8] W. Henderson, L.J. McCaffery, B.K. Nicholson, Polyhedron 17 (1998) 4291.
[9] D.J.F. Bryce, P.J. Dyson, B.K. Nicholson, D.G. Parker, Polyhedron 17 (1998) 2899.
[10] W. Henderson, J.S. McIndoe, B.K. Nicholson, P.J. Dyson, Chem. Commum. (1996) 1183.
[11] S. Konig, C. Bruckner, K.N. Raymond, J.A. Leary, J. Am. Chem. Soc. 9 (1998) 1099.
[12] A.W. Castleman, R.G. Keesee, Acc. Chem. Res. 19 (1986) 413.
[13] T.D. Mark, A.W. Castleman, Adv. At. Mol. Phys. 20 (1985) 65.
[14] T.D. Mark, Adv. Mass Spectrom. 13 (1995) 71.
[15] R.G. Cooks, G. Chen, P. Wong, H. Wollnik, in Encyclopedia of Applied Physics, VCH, New York, 1997, Vol. 19, p. 289.
[16] S.L. Zhou, M. Hamburger, Rapid Commum. Mass Spectrom. 10 (1996) 797.
[17] D.R. Zook, A.P. Bruins, Int. J. Mass Spectrom. Ion Processes 162 (1997) 129.
[18] D.R. Zook, A.P. Grimsrud, J. Am. Soc. Mass Spectrom. 2 (1991) 232.
[19] V.Q. Nguyen, X.G. Chen, A.L. Yergey, J. Am. Soc. Mass Spectrom. 8 (1997) 1175.
[20] G. Wang, R.B. Cole, Anal. Chem. 70 (1998) 873.
[21] M. Moini, B.L. Jones, R.M. Rogers, J. Longfei, J. Am. Soc. Mass Spectrom. 9 (1998) 977.
[22] S. Konig, H.M. Fales, J. Am. Soc. Mass Spectrom. 9 (1998) 814.
[23] P. Kebarle, L. Tang, Anal. Chem. 65 (1993) 972A.
[24] D.R. Zook, A.P. Bruins, Int. J. Mass Spectrom. Ion Processes 162 (1997) 129.
[25] J.C. Smith, S.P. Rafferty, R.E. March, C. Hao, T.R. Croley, Proceedings of the 48th ASMS Conference on Mass Spectrometry and Allied Topics, Long Beach CA, 2000.
[26] D. Zhang, R.G. Cooks, Int. J. Mass Spectrom. 195/196 (2000) 667.
[27] J.E. Campana, B.N. Green, Int. J. Mass Spectrom. Ion Processes 55 (1984) 281.
[28] T.M. Barlak, J.E. Campana, J.R. Wyatt, R J. Colton, J. Phys. Chem. 87 (1983) 3441.
[29] T.M. Barlak, J.E. Campana, R.J. Colton, J.J. DeCorpo, J.R. Wyatt, J. Phys. Chem. 85 (1981) 3840.
[30] T.M. Barlak, J.R. Wyatt, R.J. Colton, J.J. DeCorpo, J.E. Campana, J. Am. Chem. Soc. 104 (1982) 1212.
[31] J.A. Taylor, J.W. Rabalais, Surf. Sci. 74 (1978) 229.
[32] F. Honda, G.M. Lancaster, Y. Fukuda, J.W. Rabalais, Int. J. Mass Spectrom. Ion Phys. 32 (1978) 363.
[33] M.J. Van Stipdonk, W.R. Ferrell, D.R. Justes, R.D. English, E.A. Schweikert, Int. J. Mass Spectrom., in press.
[34] L. Drahos, R.M.A. Heeren, C. Collette, E. De Pauw, K. Vekey, J. Mass Spectrom. 34 (1999) 1373.
[35] S.A. McLuckey, D.E. Goeringer, J. Mass Spectrom. 32 (1997) 461, and references therein.
[36] R.N. Rosenfeld, J.M. Jasinski, J.I. Brauman, J. Am. Chem. Soc. 101 (1979) 3999.
[37] D. Lupo, M. Quack, Chem. Rev. 87 (1987) 181.
[38] J.M. Jasinski, R.N. Rosenfeld, F.K. Meyer, J.I. Brauman, J. Am. Chem. Soc. 104 (1982) 652.
[39] W. Tumas, R.F. Foster, M.J. Pellerite, J.I. Brauman, J. Am. Chem. Soc. 105 (1983) 7464.
[40] C.H. Watson G. Baykut, J.R. Eyler, Anal, Chem. 59 (1987) 1133.
[41] G.T. Uechi, R.C. Dunbar, J. Chem. Phys. 96 (1992) 8897.
[42] R.J. Hughes, R.E. March, A.B. Young, Int. J. Mass Spectrom. Ion Phys. 42 (1982) 255.
[43] A. Colorado, J.X. Shen, V.H. Vartanian, J. Broadbelt, Anal. Chem. 68 (1996) 4033.
[44] D.S. Tonner, D. Thölmann, T.B. McMahon, Chem. Phys. Lett. 233 (1995) 324.
[45] R.C. Dunbar, J. Phys. Chem. 98 (1994) 8705.
[46] R.C. Dunbar, T.B. McMahon, D. Thölmann, D.S. Tonner, D.R. Salahub, D. Wei, J. Am. Chem. Soc. 117 (1995) 12819.
[47] W.D. Price, P.D. Schnier, E.R. Williams, Anal. Chem. 68 (1996) 859.
[48] P.D. Schnier, W.D. Price, R.A. Jockusch, E.R. Williams, J. Am. Chem. Soc. 118 (1996) 7178.
[49] W.D. Price, P.D. Schier, R.A. Jockusch, E.F. Strittmatter, E.R. Williams, J. Am. Chem. Soc. 118 (1996) 10640.
[50] R. Orlando, C. Fenselau, R.J. Cotter, J. Am. Soc. Mass Spectrom. 2 (1991) 189.
[51] J. Gronowska, C. Paradisi, P. Traldi, U. Vettori, Rapid Commun. Mass Spectrom. 4 (1990) 306.
[52] M.J. Charles, S.A. McLuckey, G.L. Glish, J. Am. Soc. Mass Spectrom. 5 (1994) 1031.
[53] K.J. Hart, S.A. McLuckey, J. Am. Soc. Mass Spectrom. 5 (1994) 250.
[54] A. Colorado, J. Broadbelt, J. Am. Soc. Mass Spectrom. 7 (1996) 1116.
[55] J.W. Gauthier, T.R. Trautman, D.B. Jacobson, Anal. Chim. Acta 246 (1991) 211.
[56] C.S. Maier, X. Yan, M.E. Harder, M.I. Schimerkik M.L. Deinzer, L. Paša-Tolíc, R.D. Smith, J. Am. Soc. Mass Spectrom. 11 (2000) 237.
[57] K.A. Boerling, J. Rolfe, J.I. Brauman, Rapid Commum. Mass Spectrom. 6 (1992) 303.
[58] K.A. Boerling, J. Rolfe, J.I. Brauman, Int. J. Mass Spectrom. Ion Processes 117 (1993) 357.

[59] M. Busman, A.L. Rockwook, R.D. Smith, J. Phys. Chem. 96 (1992) 2397.
[60] J.E. Campana, T. M. Barlak, R.J. Colton, J.J. DeCorpo, J.R. Wyatt, B.I. Dunlop, Phys. Rev. Lett. 47 (1981) 1046.
[61] T.P. Martin, J. Chem. Phys. 72 (1980) 3506.
[62] D.E. Clemmer, M.F. Jarrold, J. Mass Spectrom. 32 (1997) 577.
[63] R. March, R. Hughes, Quadrupole Storage Mass Spectrometry, Wiley, New York, 1989, p. 77.
[64] K.X. Wan, M.L. Gross, T. Shibue, J. Am. Soc. Mass Spectrom. 11 (2000) 450.
[65] V. Grabelica, E. De Pauw, F. Rosu, J. Mass Spectrom. 34 (1999) 1328.
[66] M.J. Van Stipdonk, D.R. Justes, R.D. English, E.A. Schweikert, J. Mass Spectrom. 34 (1999) 677.
[67] S. Wei, A.W. Castleman, Int. J. Mass Spectrom. Ion Processes 131 (1994) 233.